Mixing-demixing transition and collapse of a vortex state in a quasi-two-dimensional boson-fermion mixture

Sadhan K. Adhikari[1,*] and Luca Salasnich[2,†]
[1]*Instituto de Física Teórica, UNESP–São Paulo State University, 01.405-900 São Paulo, São Paulo, Brazil*
[2]*CNISM and CNR-INFM, Unità di Padova, Dipartimento di Fisica "Galileo Galilei," Università di Padova, Via Marzolo 8, 35131 Padova, Italy*
(Received 20 December 2006; published 8 May 2007)

We investigate the mixing-demixing transition and the collapse in a quasi-two-dimensional degenerate boson-fermion mixture (DBFM) with a bosonic vortex. We solve numerically a quantum-hydrodynamic model based on a new density functional which accurately takes into account the dimensional crossover. It is demonstrated that with the increase of interspecies repulsion, a mixed state of DBFM could turn into a demixed state. The system collapses for interspecies attraction above a critical value which depends on the vortex quantum number. For interspecies attraction just below this critical limit there is almost complete mixing of boson and fermion components. Such mixed and demixed states of a DBFM could be experimentally realized by varying an external magnetic field near a boson-fermion Feshbach resonance, which will result in a continuous variation of interspecies interaction.

DOI: 10.1103/PhysRevA.75.053603 PACS number(s): 03.75.Lm, 03.75.Ss

I. INTRODUCTION

A quantum degenerate Fermi gas (DFG) cannot be achieved by evaporative cooling due to a strong repulsive Pauli-blocking interaction at low energies among spin-polarized fermions [1]. Trapped DFG has been achieved only by sympathetic cooling in the presence of a second boson or fermion component. Recently, there have been successful observation [1–4] and associated experimental [5–7] and theoretical [8–16] studies of degenerate boson-fermion mixtures by different experimental groups [1–4] in the following systems: ^{7}Li-^{6}Li [3], ^{23}Na-^{6}Li [4], and ^{87}Rb-^{40}K [5,6]. Moreover, there have been studies of a degenerate mixture of two components of fermionic ^{40}K [1] and ^{6}Li [2] atoms. The collapse of the DFG in a degenerate boson-fermion mixture (DBFM) of ^{87}Rb-^{40}K has been observed and studied by Modugno *et al.* [5,13,16], and has also been predicted in a degenerate fermion-fermion mixture of different-mass atoms [17].

Several theoretical investigations [9,11,12] of a trapped DBFM considered the phenomenon of the mixing-demixing transition in a state of zero angular momentum when the boson-fermion repulsion is increased. For a weak boson-fermion repulsion both a Bose-Einstein condensate (BEC) and a DFG have maxima of probability density at the center of the harmonic trap. However, with the increase of boson-fermion repulsion, the maximum of the probability density of the DFG could be slowly expelled from the central region. With further increase of boson-fermion repulsion, the DFG could be completely expelled from the central region which will house only the BEC. This phenomenon has been termed the mixing-demixing transition in a DBFM. The phenomenon of demixing has drawn some attention lately as in a demixed state an exotic configuration of the mixture is formed, where there is practically no overlap between the two components and one can be observed and studied independent of the other. It has been argued [9] that such a demixed state in a DBFM should be possible experimentally by increasing the interspecies scattering length near a Feshbach resonance [18]. More recently the mixing-demixing transition has been studied in a degenerate fermion-fermion mixture [19].

On the other hand, if the interspecies interaction is turned attractive and its strength increased, the DBFM collapses above a critical strength. There has been several experimental [5,20,21] and theoretical [8,13,16] studies of collapse in a DBFM of ^{40}K-^{87}Rb mixture. As the interaction in a pure DFG at short distances is repulsive due to Pauli blocking, there cannot be a collapse in it. A collapse is possible in a DBFM in the presence of a sufficiently strong Boson-fermion attraction which can overcome the Pauli repulsion among identical fermions [5].

It is pertinent to see how the mixing-demixing transitions manifest for interspecies attraction below the critical value for collapse. The appearance of a quantized bosonic vortex state is the genuine confirmation of superfluidity in a trapped BEC. In view of many experimental studies of such bosonic vortex states it is also of interest to see how the mixing-demixing phenomenon in a DBFM modify in the presence of a bosonic vortex. The vortices are quantized rotational excitations [22] and can be observed in two-dimensional (2D) systems. The lowest of such excitations with unit angular momentum ($\hbar$) per atom is the nonlinear extension of a well-understood linear quantum state [23]. Vortex states in a BEC have been observed experimentally [24]. Different techniques for creating vortex states in BEC have been suggested [25], e.g., stirring the BEC with an external laser [26], forming spontaneously in evaporative cooling [27], using a "phase imprinting method" [28], and rotating an axially symmetric trap [29]. Recently, the stability of the vortex state and

*Electronic address: adhikari@ift.unesp.br; URL: http://www.ift.unesp.br/users/adhikari
†Electronic address: salasnich@pd.infn.it; URL: http://www.padova.infm.it/salasnich

the formation of persistent currents have been theoretically analyzed also in toroidal traps [30–32]. The generation of vortex in degenerate fermions is much more complex [33] and we shall not consider this possibility here.

The purpose of this paper is to study and illustrate the mixing-demixing phenomenon for both attractive and repulsive interspecies interaction in a trapped DBFM vortex in a quasi-2D configuration using a quantum-hydrodynamic model inspired by the success of this model in the investigation of fermionic collapse [16] and bright [34,35] and dark [36] solitons in a DBFM. The conclusions of the study on bright soliton [35] are in agreement with a microscopic study [37], and those on collapse [16] are in agreement with experiments [5,20]. This time-dependent mean-field-hydrodynamic model was suggested recently [16] to study the collapse dynamics of a DBFM.

In addition to the study of the mixing-demixing transition in a DBFM in a quasi-2D configuration, we also study conditions of stability and collapse in it. Specifically, we study the conditions of stability when the parameters of a DBFM are modified, e.g., boson-boson and boson-fermion interactions as well as the boson and fermion numbers.

There have been prior investigations of the mixing-demixing transition [11,12] in a trapped DBFM upon an increase of interspecies repulsion. Also, there have been previous investigations of stability and collapse [13,15] in a trapped DBFM. In contrast to these previous time-independent studies for stationary states, the present study relies on a time-dependent formulation and investigates the mixing-demixing transition and stability and collapse for both attractive and repulsive interspecies interaction and extends to the case of vortex states.

The model hydrodynamic equations in a quasi-2D form is derived from a Lagrangian density for the DBFM where the boson Lagrangian is taken in the usual mean-field Gross-Pitaevskii form [38]. The interaction Lagrangian between bosons and fermions is also taken to have the standard product form of boson and fermion probability densities. We derive a new Lagrangian for the quasi-2D fermions by putting them in a box of length L along x and y directions and in a harmonic potential well along z direction. By occupying the lowest single-particle fermion states we calculate the fermion probability density as a function of chemical potential from which we obtain the corresponding fermion Lagrangian density. The resultant hydrodynamic equations have a nonpolynomial nonlinearity for the fermions, which we use in our calculation. In the strict 2D limit, when axial excitations are not allowed, this nonlinearity reduced to a standard cubic form.

The paper is organized as follows. In Sec. II we present an account of the quantum hydrodynamic model consisting of a set of coupled partial differential equations involving a quasi-2D BEC and a DFG. In Sec. III we present the numerical results on the mixing-demixing transition and collapse of a DBFM in two subsections, respectively. In Sec. IV we present a summary and discussion. Some technical details are given in the Appendix.

II. BOSON-FERMION LAGRANGIAN FOR QUASI-2D HYDRODYNAMICS

We consider a DBFM with N_B Bose-condensed atoms of mass m_B and N_F spin-polarized fermions of mass m_F at zero temperature. A natural choice for a quasi-2D trap-geometry is a very strong confinement along the z axis: in this axial direction we choose a harmonic potential of frequency ω_z. In the cylindric radial directions we take two generic external potentials for bosons and fermions: $V_B(\rho)$ and $V_F(\rho)$, where $\rho=(x^2+y^2)^{1/2}$ is the cylindric radial coordinate.

To describe this quasi-2D DBFM we use two dynamical fields $\psi_B(\rho,t)$ and $\psi_F(\rho,t)$. The complex function $\psi_B(\rho,t)$ is the hydrodynamic field of the Bose gas, such that $n_B=|\psi_B|^2$ is the 2D bosonic probability density and $v_B=i\partial_\rho \ln(\psi_B/|\psi_B|)$ is the bosonic velocity. The complex function $\psi_F(\rho,t)$ is the hydrodynamic field of the Fermi gas, such that $n_F=|\psi_F|^2$ is the 2D fermionic density and $v_F=i\partial_\rho \ln(\psi_F/|\psi_F|)$ is the fermionic velocity. These two complex fields are the Lagrangian variables of the Lagrangian density

$$\mathcal{L}=\mathcal{L}_B+\mathcal{L}_F+\mathcal{L}_{BF}, \tag{1}$$

where $\mathcal{L}_B$ is the bosonic Lagrangian, $\mathcal{L}_F$ is the fermionic Lagrangian, and $\mathcal{L}_{BF}$ is the Lagrangian of the boson-fermion interaction. It is important to stress that in our model, based on quantum hydrodynamics [38,39], the bosonic Lagrangian $\mathcal{L}_B$ describes very accurately all the dynamical properties of the dilute quasi-2D BEC [39,40], while the fermionic Lagrangian $\mathcal{L}_F$ can be safely used only for static and collective properties of the quasi-2D Fermi gas [39]. Note that recently quantum hydrodynamics has been also successfully applied to investigate the dimensional crossover from a 3D BEC to a 1D Tonks-Girardeau gas [41,42] in a DBFM.

The bosonic Lagrangian is given by [16,35,40]

$$\mathcal{L}_B=\frac{i\hbar}{2}(\psi_B^*\partial_t\psi_B-\psi_B\partial_t\psi_B^*)-\frac{\hbar^2}{2m_B}|\nabla_\rho\psi_B|^2-\frac{\hbar^2l^2}{2m_B\rho^2}n_B-\mathcal{E}_B(n_B)-V_Bn_B, \tag{2}$$

where $\hbar^2l^2/(2m_B\rho^2)$ is the centrifugal term of the bosonic vortex, l is the integer quantum number of circulation, and $\hbar l$ is the angular momentum of each atom in the axial (z) direction [23]. The term $\mathcal{E}_B(n_B)$ is the bulk energy density of the dilute and interacting quasi-2D BEC under axial harmonic confinement. As shown in Ref. [40], this bulk energy density is a nonpolynomial function of the 2D bosonic density $n_B=|\psi_B|^2$. For small bosonic densities, i.e., for $0\leqslant n_B<1/(2\sqrt{2\pi}a_{BB}a_{zB})$ where a_{BB} is the 3D Bose-Bose scattering length and $a_{zB}=\sqrt{\hbar/(m_B\omega_z)}$ is the characteristic length of axial harmonic confinement for bosons, the BEC is strictly 2D and one finds

$$\mathcal{E}_B=\frac{1}{2}g_{BB}n_B^2, \tag{3}$$

where $g_{BB}=4\pi\hbar^2a_{BB}/(\sqrt{2\pi}a_{zB}m_B)$ is the 2D interatomic strength [40]. For very large densities, i.e., for $n_B\gg 1/(2\sqrt{2\pi}a_{BB}a_{zB})$, the BEC is instead 3D and $\mathcal{E}_B$ scales as $n_B^{5/3}$ (for details see Ref. [40], where nonpolynomial

Schrödinger equations are derived for cigar-shaped and disk-shaped BECs starting from the 3D Gross-Pitaevskii Lagrangian). Here we consider a BEC with a small a_{zB} (strong axial confinement) and a much smaller scattering length a_{BB} and so the BEC is strictly 2D.

The fermionic Lagrangian is given by [16,35]

$$\mathcal{L}_F = \frac{i\hbar}{2}(\psi_F^* \partial_t \psi_F - \psi_F \partial_t \psi_F^*) - \frac{\hbar^2}{6m_F}|\nabla_\rho \psi_F|^2 - \mathcal{E}_F(n_F) - V_F n_F, \tag{4}$$

where $\mathcal{E}_F(n_F)$ is the bulk energy density of a noninteracting quasi-2D Fermi gas at zero temperature and under axial harmonic confinement. As shown in the Appendix, this bulk energy density is a nonpolynomial function of the 2D fermionic density $n_F=|\psi_F|^2$. For small fermionic densities, i.e., for $0 \leqslant n_F < 1/(2\pi a_{zF}^2)$, the Fermi gas is strictly 2D and one finds $\mathcal{E}_F=\hbar\omega_z \pi (a_{zF} n_F)^2$, where $a_{zF}=\sqrt{\hbar/(\omega_z m_F)}$ is the characteristic length of axial harmonic confinement of fermions. For large densities, i.e., for $n_F \gg 1/(2\pi a_{zF}^2)$, the Fermi gas is 3D and, as shown in the Appendix, one has $\mathcal{E}_F = (4a_{zF}^3\sqrt{\pi}/3)(\hbar\omega_z) n_F^{3/2}$. Contrary to the case of bosons, whose dimensionality depends also on a_{BB} (that is very small), for fermions it is necessary to use an extremely small a_{zF} and a very small number of atoms to have a strictly 2D configuration. This is not the case of real experiments and so we use the formula

$$\mathcal{E}_F = \frac{\hbar\omega_z}{a_{zF}^2}\begin{cases} \pi(n_F a_{zF}^2)^2 & \text{for } 0 \leqslant n_F a_{zF}^2 < \dfrac{1}{2\pi}, \\ \dfrac{1}{6\pi}(4\pi n_F a_{zF}^2 - 1)^{3/2} + \dfrac{1}{12\pi} & \text{for } n_F a_{zF}^2 \geqslant \dfrac{1}{2\pi}, \end{cases} \tag{5}$$

which has been deduced in the Appendix and gives the full 2D-3D crossover of an ideal Fermi gas that is uniform in the cylindric radial direction and under harmonic confinement in the cylindric axial direction. It is interesting to stress that the study of 2D-3D (and 1D-3D) cross overs have a long history in trapped (bosonic) atoms. There have been careful studies of a pair of trapped atoms [43] as well as of a large number of trapped atoms [44]. In the Appendix we consider a different type of the 2D-3D crossover for a large number of ideal Fermi gas atoms distributed over different quantum states obeying the Pauli principle.

In the fermionic Lagrangian of Eq. (4) the Weiszäcker gradient term $-\hbar^2|\nabla_\rho \psi_F|^2/(6m_F)$ takes into account the additional kinetic energy due to spatial variation [14] but contributes little to this problem compared to the dominating Pauli-blocking term $\mathcal{E}_F(n_F)$ [45,46] for a large number of Fermi atoms. The interaction between intra-species fermions in the spin-polarized state is highly suppressed due to the Pauli-blocking term and has been neglected in the Lagrangian $\mathcal{L}_F$ and will be neglected throughout.

Finally, the Lagrangian of the boson-fermion interaction reads [14,47]

$$\mathcal{L}_{BF} = -g_{BF} n_B n_F, \tag{6}$$

where $g_{BF}=2\pi\hbar^2 a_{BF}/(m_R\sqrt{2\pi a_{zB} a_{zF}})$ with a_{BF} the 3D Bose-Fermi scattering length and $m_R=m_B m_F/(m_B+m_F)$ the Bose-Fermi reduced mass.

The Euler-Lagrange equations of motion of the Lagrangian density (1) with Eqs. (2), (4), and (6) are given by

$$i\hbar\frac{\partial}{\partial t}\psi_B = \left[-\frac{\hbar^2\nabla_\rho^2}{2m_B} + \frac{\hbar^2 l^2}{2m_B\rho^2} + \mu_B(n_B) + V_B + g_{BF} n_F\right]\psi_B, \tag{7}$$

$$i\hbar\frac{\partial}{\partial t}\psi_F = \left[-\frac{\hbar^2\nabla_\rho^2}{6m_F} + \mu_F(n_F) + V_F + g_{BF} n_B\right]\psi_F, \tag{8}$$

where $\mu_B=\partial\mathcal{E}_B/\partial n_B = g_{BB} n_B$ is the bulk chemical potential of the strictly 2D BEC and $\mu_F=\partial\mathcal{E}_F/\partial n_F$ is the bulk chemical potential, given by Eq. (A8) in the Appendix, of the ideal Fermi gas in the 2D-3D crossover. The normalization used in Eqs. (7) and (8) and above is $2\pi\int_0^\infty |\psi_j|^2 \rho d\rho = N_j$.

For $g_{BF}=0$ Eq. (7) is the 2D Gross-Pitaevskii equation while Eq. (8) is essentially a time-dependent generalization of a quasi-2D version of the time-independent equations of motions suggested by Capuzzi *et al.* [14] and Minguzzi *et al.* [15] to study static and collective properties of a confined, dilute, and spin-polarized Fermi gas. That time-independent version was a generalization of the Thomas-Fermi (TF) approximation for the density of a Fermi gas [45]. The TF approximation for a stationary Fermi gas can be obtained from Eq. (8) by setting the kinetic energy term to zero. For a large number of Fermi atoms, in Eq. (8) the nonlinear term $\mu_F(n_F)$ is much larger than the kinetic energy term, hence the inclusion of the kinetic energy in Eq. (8) changes the probability amplitude ψ_F only marginally. However, inclusion of the kinetic energy in Eq. (8) has the advantage of leading to a probability amplitude ψ_F analytic in space variable ρ, whereas the TF approximation is not analytic in ρ [35].

As previously discussed, the Lagrangian (1) with Eqs. (2), (4), and (6) describes a DBFM under axial harmonic confinement of frequency ω_z and any kind of the external potentials $V_B(\rho)$ and $V_F(\rho)$ in the cylindric radial directions. For our investigation of bosonic vortices in presence of fermions we take the following radial traps:

$$V_B(\rho) = V_F(\rho) = \frac{1}{2} m_B \omega_\perp^2 \rho^2, \tag{9}$$

as in the study by Modugno *et al.* [13] and Jezek *et al.* [45], where $\omega_\perp$ refer to the trap frequency for bosons. In this way the quasi-2D mixture is achieved from the so-called disk-shaped configuration: the DBFM is confined by an anisotropic 3D harmonic potential $V(\mathbf{r})=\frac{1}{2}m_B\omega_\perp^2(\rho^2+\lambda^2 z^2)$, where $\lambda=\omega_z/\omega_\perp$ is the trap anisotropy. The quasi-2D configuration is appropriate for studying vortices in the disk-shaped geometry with anisotropy parameter $\lambda \gg 1$.

III. NUMERICAL RESULT

The main numerical advantage of working with Eqs. (7) and (8) is that the calculations are much faster. In fact, one

has to solve the two coupled differential equations with only one space variable ρ. The full 3D problem will require an enormous computational effort. In our numerical simulation we consider the ^{40}K-^{87}Rb mixture and take $\lambda=10$, $\omega_z=2\pi\times100$ Hz. We take m_B as the mass of ^{87}Rb and m_F as the mass of ^{40}K.

We solve numerically the coupled quantum-hydrodynamic equations (7) and (8) for vortex quantum numbers $l=0$ and $l=1$ by using a imaginary-time propagation method based on the finite-difference Crank-Nicholson discretization scheme elaborated in Ref. [48]. In this way we obtain the ground-state of the DBFM at a fixed value of the vortex quantum number l. We discretize the quantum-hydrodynamics equations (7) and (8) using time step 0.0003 ms and space step 0.02 μm.

The scattering length a_{BF} is varied from positive (repulsive) to negative (attractive) values through zero (noninteracting). Note that in the experiments the scattering length a_{BF} can be manipulated in ^{6}Li-^{23}Na and ^{40}K-^{87}Rb mixtures near recently discovered Feshbach resonances [18] by varying a background magnetic field.

A. Mixing-demixing transition

In the first part of our numerical investigation we consider the mixing-demixing transition in the quasi-2D DBFM with vortex quantum number $l=0,1$. For a sufficiently large repulsive a_{BF} there is demixing and for a large attractive a_{BF} there is mixing. If the attractive a_{BF} is further increased there could be collapse in the DBFM, which we study in detail in the next subsection. The mixing-demixing phenomenon is quite similar for various boson and fermion numbers and we illustrate it choosing $N_F=120$, $N_B=1000$, and $a_{BB}=40$ nm.

The results of our imaginary-time calculation with vortex quantum number $l=0$ are shown in Fig. 1, where we plot the probability density $|\psi_j|^2$ vs cylindric radii ρ of the stationary boson-fermion mixture in a quasi-2D configuration for noninteracting, repulsive and attractive interspecies interaction. The probability density in Figs. 1 and 2 is normalized to unity: $2\pi\int_0^\infty|\psi_j|^2\rho d\rho=1$. In all cases, with $a_{BF}>0$, because of the large nonlinear Pauli-blocking fermionic repulsion, the fermionic profile extends over a larger region of space than the bosonic one. As shown in Fig. 1, in agreement with previous studies in the $l=0$ state, a complete mixing-demixing transition is found by increasing a_{BF} from $a_{BF}=0$ to $a_{BF}=100$ nm. Instead, in the case of attractive boson-fermion interaction ($a_{BF}<0$) we find that the fermionic cloud is pulled inside the bosonic one and a complete overlap between the two clouds is then achieved. With further increase in boson-fermion interaction the system collapses. In Fig. 1(d), where $a_{BF}=-30$ nm, just below the critical value for collapse, we find an almost complete mixing between the bosonic and fermionic components.

In the second part of the investigation we consider a BEC with vortex quantum number $l=1$ in a DBFM with the same parameters of Fig. 1. The results are displayed in Fig. 2. The noninteracting case ($a_{BF}=0$) is exhibited in Fig. 2(a) with $N_F=120$, $N_B=1000$, $a_{BB}=40$ nm. The fermionic profile in this case is quite similar to that in the $l=0$ state exhibited in Fig. 1(a). However, the bosonic profile has developed a dip near origin due to the $l=0$ vortex state. In Fig. 2(b) upon introducing a interspecies repulsion between bosons and fer-

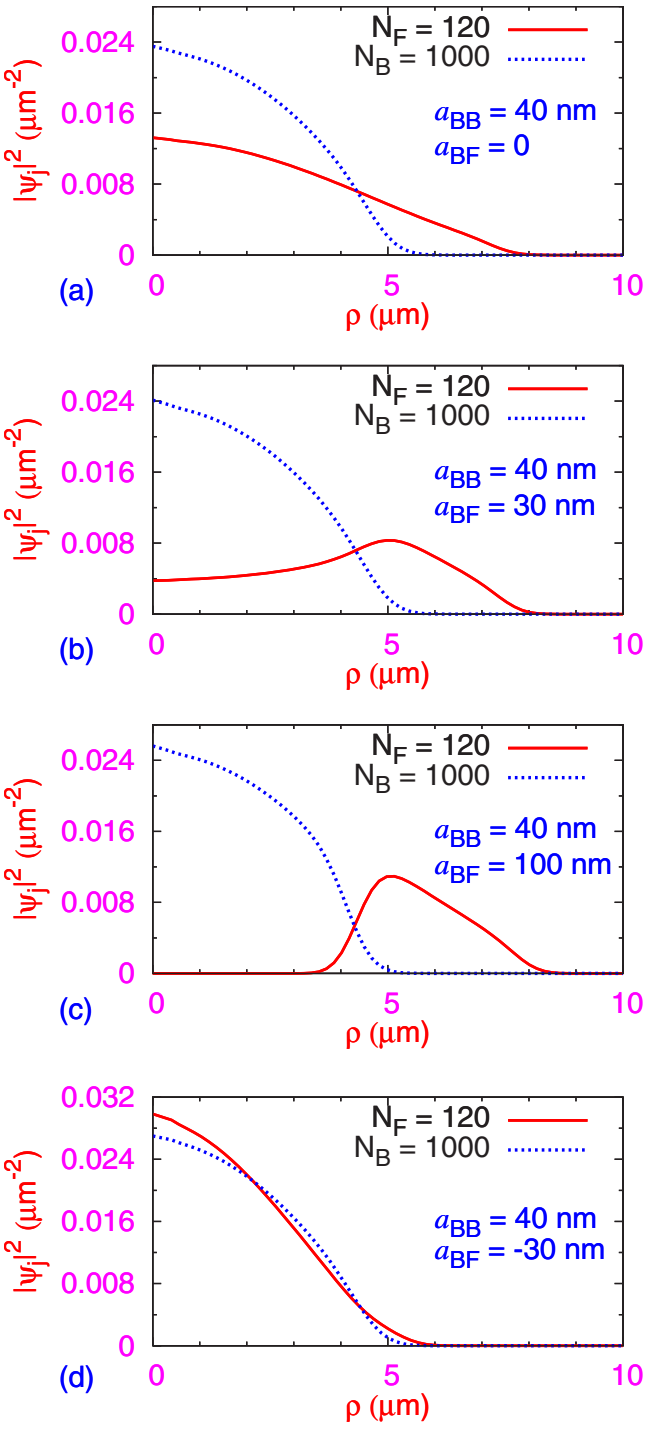

FIG. 1. (Color online) DBFM with BEC having vortex quantum number $l=0$. Probability densities $|\psi_j|^2$ of bosons and fermions as a function of the cylindric radial coordinate ρ. N_B(=1000) and N_F(=120) are the numbers of bosons and fermions, respectively. The trap anisotropy is $\lambda=10$ The four panels correspond to different values of the Bose-Fermi scattering length a_{BF}(=0, 30 nm, 100 nm, −30 nm) and fixed Bose-Bose scattering length a_{BB}(=40 nm). Note that in panel (d) a_{BF} is negative.

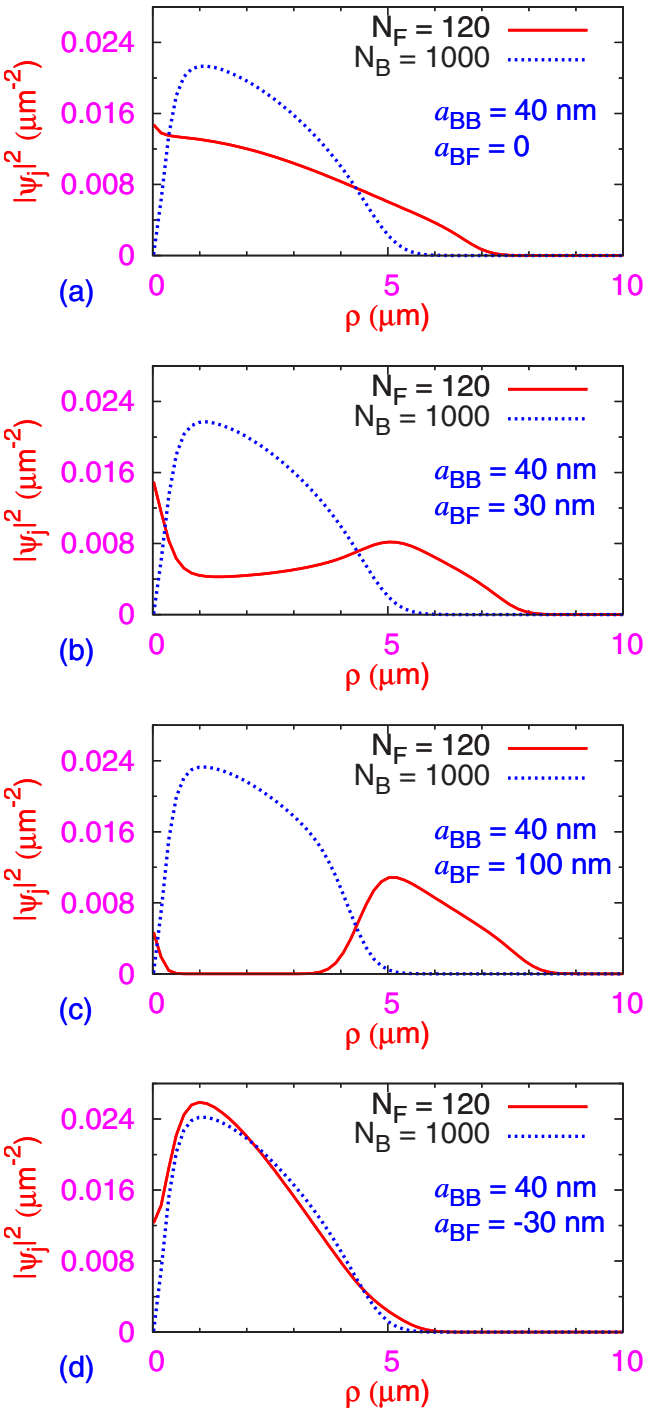

FIG. 2. (Color online) DBFM with BEC having vortex quantum number $l=1$. Probability densities $|\psi_j|^2$ of bosons and fermions as a function of the cylindric radial coordinate ρ. Parameters as in Fig. 1.

mions a demixing has started and the fermionic wave function is partially pushed out from the central region for $a_{BF}=30$ nm. This demixing has increased in Fig. 2(c) for $a_{BF}=100$ nm. The fermionic profile in Fig. 2(c) for the vortex state with $l=1$ is quite similar to the corresponding state in Fig. 1(c) for $l=0$. Finally, we find that an attractive boson-fermion interaction increases the mixing of boson and fermion components and the mixing is maximum for a critical

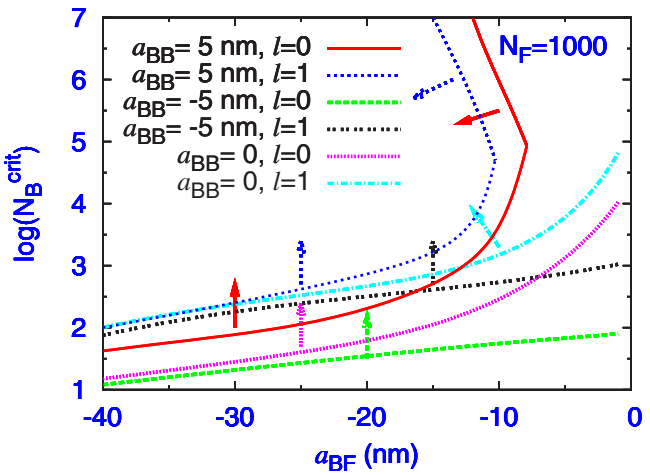

FIG. 3. (Color online) Critical number N_B^{crit} of bosons vs Bose-Fermi scattering length a_{BF} in the DBFM. The number N_F of fermions is fixed at 1000. Vortex quantum number l and Bose-Bose scattering length a_{BB} are instead varied. The region of collapse is indicated by arrows.

value of a_{BF} before the occurrence of collapse in the DBFM. The boson and fermion profiles for $a_{BF}=-30$ nm just below the threshold for collapse is shown in Fig. 2(d). In this case the mixing is so perfect that the fermionic profile has developed a central dip near $\rho=0$ reminiscent of a vortex state as in the bosonic component. However, near $\rho=0$ the fermionic wave function $\psi_F(\rho)$ tends to a constant value and does not have the vortex state behavior $\psi_B(\rho)\sim\rho^l$. This shows that the fermionic state is not really a vortex but due to mixing it tends to simulate one.

B. Stability and collapse

For given values of N_B, N_F, a_{BB}, and angular momentum l, a stable configuration is always achieved for a repulsive (positive) a_{BF}. However, for a sufficiently large attractive (negative) a_{BF}, the system collapses as the overall attractive interaction between bosons and fermions supersedes the overall stabilizing repulsion of the system thus leading to instability. Also, alternatively, for a fixed a_{BF}, N_F, a_{BB} and angular momentum l, the system may collapse for N_B greater than a critical value N_B^{crit}. This may happen for all values of the parameters and a typical situation is illustrated in Fig. 3, where we plot N_B^{crit} vs a_{BF} in different cases for $N_F=1000$. One can have collapse in a single or both components. After collapse the radius of the system reduces to a very small value.

For $a_{BB}\leqslant 0$ the system is stable for $N<N_B^{\text{crit}}$ for both $l=0$ and 1 as one can see from Fig. 3, where we plot results for $a_{BB}=0$ and -5 nm. The region of instability and collapse is indicated by arrows for $N>N_B^{\text{crit}}$. In Fig. 3 we find that the region of stability has increased after the inclusion of the angular momentum term. Due to the stabilizing repulsive centrifugal term $\hbar^2 l^2/(2m_B\rho^2)$ the rotating ($l=1$) DBFM is more stable than the nonrotating ($l=0$) one [49].

For $a_{BB}>0$, the bosons have a net repulsive energy and the system does not collapse unless the strength of boson-

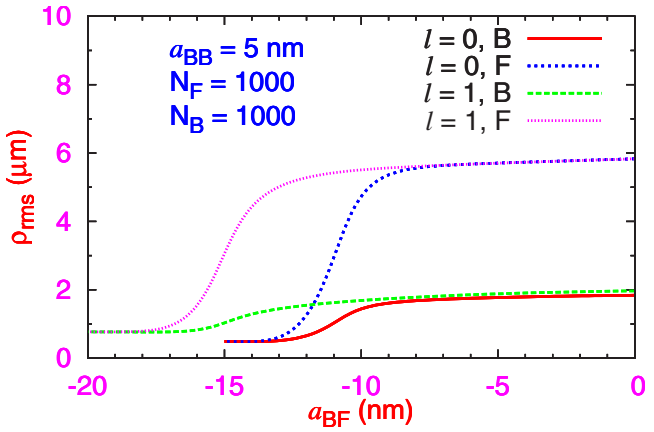

FIG. 4. (Color online) Root mean square radius $\rho_{\rm rms}$ of the two clouds in the DBFM as a function of the Bose-Fermi scattering length a_{BF}. Here the number N_B of bosons (labeled B) is equal to the number N_F of fermions (labeled F) fixed at 1000. The results are shown for two values of the BEC vortex quantum number $l=0,1$.

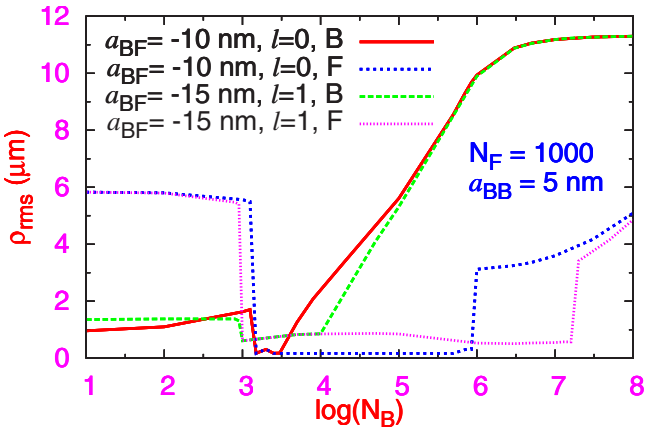

FIG. 5. (Color online) Root mean square radius $\rho_{\rm rms}$ of the two clouds in the DBFM as a function of $\ln(N_B)$, that is the logarithm of the number N_B of bosons (labeled B). Here the number N_F of fermions (labeled F) is fixed at 1000. The results are show for two values of the BEC vortex quantum number $l=0,1$.

fermion attraction $|a_{BF}|$ is increased beyond a critical value. In this situation an interesting scenario appears at fixed a_{BF}, a_{BB}, N_F, and l, as N_B is increased. Increasing N_B from a small value past the critical value $N_B^{\rm crit}$, the system collapses because the attractive interaction in the Lagrangian density (6) becomes large enough to overcome the stabilizing repulsions in boson-boson and fermion-fermion subsystems. However, when N_B becomes very large ($N_B \gg N_F$) past a second critical value, the attractive interaction in the Lagrangian density (6) will become small compared to the overall repulsion of the system and a stable configuration can again be obtained. This is clearly illustrated in Fig. 5. Note that, in Eq. (6), $|\psi_B|^2 \propto N_B$ and $|\psi_F|^2 \propto N_F$ and for a fixed total number of atoms (N_B+N_F) $\mathcal{L}_{BF}$ becomes large for $N_B \approx N_F$ and small for $N_B \gg N_F$ or $N_B \ll N_F$. Hence, a small number N_F of fermions should not destabilize the stable configuration of a large number N_B of repulsive bosons. Similarly, a small number N_B of bosons should not destabilize the stable configuration of a large number N_F of repulsive fermions. This feature, that is explicitly shown in Fig. 3, should be quite general independent of dimensionality of space. It is not clear why this feature was not found in the 3D theoretical study of Ref. [8].

Next we analyze how the system moves towards collapse as the parameters of the model are changed. First we consider the passage to collapse as the attractive strength of boson-fermion interaction is increased. To see this we plot the root-mean-square (rms) radii $\rho_{\rm rms}$ of bosons and fermions vs a_{BF} in several cases in Fig. 4. The rms radii remain fairly constant away from the region of collapse. However, as a_{BF} approaches the value for collapse the rms radii decrease rapidly to a small value signalling the collapse. In this case both bosons and fermions experience collapse simultaneously.

We also studied the collapse for a fixed attractive a_{BF}, a_{BB}, and N_F, while N_B is varied, to demonstrate that stable configuration can be attained simultaneously for bosons and fermions for small and large N_B, e.g., for $N_B \ll N_F$ or $N_B \gg N_F$. For intermediate N_B there is collapse in either bosons or fermions or both. This is illustrated in Fig. 5 where we plot $\rho_{\rm rms}$ vs $\ln(N_B)$ for $N_F=1000$ and $a_{BB}=5$ nm for both bosons and fermions for $l=0$ and 1. In both cases ($l=0,1$), as N_B is increased from a small value, the collapse is initiated near $N_B=N_B^{\rm crit} \approx 1000$ when the radii of both bosons and fermions suddenly drop to a small value signalling a collapse in both subsystems. With further increase in N_B near $N_B \approx 8000$ the bosons pass to a stable state from a collapsed state and the corresponding rms radii increase with N_B. The fermions continue in a collapsed state with a small radii. However, near $N_B \approx 5\times 10^6$ the fermions also come out of the collapsed state and with the increase of N_B the fermion radius starts to increase. For $N_B > 10^7$, a stable configuration of the DBFM is obtained as the boson-boson and fermion-fermion repulsion compensates for the boson-fermion attraction.

IV. CONCLUSION

We have used a coupled set of quantum-hydrodynamic equations to study the mixing-demixing transition as well as stability and collapse of a trapped DBFM. The model equations are solved by imaginary time propagation of the finite-difference Crank-Nicholson algorithm. In our analysis the Bose-Einstein condensate is strictly 2D while the Fermi gas is not: for this reason we have introduced a new fermionic density functional which accurately takes into account the dimensional crossover of fermions from 2D to 3D. In the study of the mixing-demixing transition we have taken the boson-boson interaction to be repulsive and the boson-fermion interaction to be both attractive and repulsive. By considering a bosonic vortex with quantum number l, we have found that in both $l=0$ and $l=1$ cases the mixing could be almost complete up to the critical value of boson-fermion attraction beyond which the system collapses. When the boson-fermion interaction is turned repulsive, there is the mixing-demixing transition which is regulated by the boson-fermion repulsion.

We have also studied the collapse in $l=0$ and $l=1$ cases. The $l=1$ system is found to be more stable due to the cen-

trifugal kinetic term. We have investigated in detail how stability is affected when the boson-boson and boson-fermion interaction as well as boson and fermion numbers are varied.

The present analysis is based on mean-field Eqs. (7) and (8) for the Bose-Fermi mixture, which are very similar in structure to those satisfied by a Bose-Bose mixture [50]. In the mean-field equations for a Bose-Bose mixture all nonlinearities are cubic in nature. In the present mean-field equations for a Bose-Fermi mixture apart from the intraspecies Fermi (diagonal) nonlinearity arising from the Pauli principle in Eq. (8), given by Eq. (A8), all other nonlinearities are also cubic in nature. In Eq. (A8) the nonlinearity is partly cubic and partly has a different form; whereas in the strict 2D limit this nonlinearity is entirely cubic in nature. Bearing such a similarity with the mean-field equations of the Bose-Bose mixture, the $l=0$ results for the mixing-demixing transition and collapse in Bose-Fermi mixture presented here are expected to be similar to those of a Bose-Bose mixture provided that the scattering lengths and trap parameters are adjusted in two cases to lead to similar strengths of the nonlinearities. (It has been demonstrated, similar to the present Bose-Fermi mixture, that a Bose-Bose mixture with intraspecies repulsion and interspecies attraction can experience collapse [50].) But the present $l=1$ results with a bosonic vortex in a Bose-Fermi mixture have no analogy with in the Bose-Bose case. A slowly rotating Bose-Fermi mixture can have a quantized bosonic vortex with $l=1$ with no vortex in the fermions; whereas a similar Bose-Bose mixture should have a $l=1$ vortex in both the bosonic components in a stable stationary configuration. Consequently, the mean-field equations satisfied by the slowly rotating Bose-Fermi mixture will be distinct from those satisfied by a slowly rotating Bose-Bose mixture and the present results for $l=1$ should be distinct from those for a Bose-Bose mixture.

The present findings can be verified in experiments on DBFMs, specially for the vortex state, thus presenting yet another critical test of our quantum-hydrodynamic model.

ACKNOWLEDGMENTS

L.S. thanks Flavio Toigo for useful discussions. The work of S.K.A. is supported in part by the CNPq and FAPESP of Brazil.

APPENDIX

In this appendix we derive the zero-temperature equations of state for an ideal Fermi gas that is uniform in the cylindric radial direction but under harmonic confinement in the cylindric axial direction. In particular we obtain the chemical potential μ_F and the energy density $\mathcal{E}_F$ as a function of the 2D uniform radial density n_F of the Fermi gas.

Let us consider an ideal Fermi gas in a box of length L along x and y axis and harmonic potential of frequency ω_z along the z axis. The total number of particles is

$$N_F = \sum_{i_x i_y i_z} \theta(\mu - \epsilon_{i_x i_y i_z}), \tag{A1}$$

where the single particle energy reads

$$\epsilon_{i_x i_y i_z} = \frac{\hbar^2}{2m_F}\frac{(2\pi)^2}{L^2}(i_x^2 + i_y^2) + \hbar\omega_z\left(i_z + \frac{1}{2}\right). \tag{A2}$$

Here i_x, i_y are integer quantum numbers and i_z is a natural quantum number. Let us approximate i_x and i_y by real numbers (see also Ref. [51]). Then

$$N_F = \sum_{i_z=0}^{\infty} \int di_x di_y \theta(\mu - \epsilon_{i_x i_y i_z}). \tag{A3}$$

Setting $k_x = \frac{2\pi}{L} i_x$ and $k_y = \frac{2\pi}{L} i_y$, the number of particles can be rewritten as

$$N_F = \sum_{i_z=0}^{\infty} \frac{L^2}{(2\pi)^2} \int dk_x dk_y \theta(\mu - \epsilon_{k_x k_y i_z}). \tag{A4}$$

The 2D density is then

$$n_F = \frac{N_F}{L^2} = \frac{1}{4\pi^2} \sum_{i_z=0}^{\infty} \int dk_x dk_y \theta(\mu - \epsilon_{k_x k_y i_z}). \tag{A5}$$

Now we rewrite the density n_F in the following way:

$$n_F = \frac{1}{4\pi^2} \int dk_x dk_y \theta(\mu - \epsilon_{k_x k_y 0}) + \frac{1}{4\pi^2} \sum_{i_z=1}^{\infty} \int dk_x dk_y \theta(\mu - \epsilon_{k_x k_y i_z}). \tag{A6}$$

The first term is the density of a strictly 2D Fermi gas (only the lowest single-particle mode along the z axis is occupied) and the second term is the density which takes into account of all single-particle modes along the z axis, apart the lowest one. Setting $k^2 = k_x^2 + k_y^2$ the first term of the density n_F can be written as

$$\frac{1}{4\pi^2} \int 2\pi k dk \theta\left(\mu - \frac{\hbar^2 k^2}{2m} - \frac{1}{2}\hbar\omega_z\right) = \frac{1}{2\pi a_{zF}^2}\left(\frac{\mu}{\hbar\omega_z} - \frac{1}{2}\right),$$

where $a_{zF} = \sqrt{\hbar/(m_F\omega_z)}$. The second term of the 2D density n_F is evaluated by transforming it to an integral and is given by

$$\sum_{i_z=1}^{\mu/\hbar\omega_z - 1/2} \frac{1}{2\pi a_{zF}^2}\left[\frac{\mu}{\hbar\omega_z} - \left(i_z + \frac{1}{2}\right)\right] = \frac{1}{4\pi a_{zF}^2}\left(\frac{\mu}{\hbar\omega_z} - \frac{3}{2}\right)^2.$$

In conclusion the 2D density n_F is given by

$$n_F = \frac{1}{2\pi a_{zF}^2}\left[\left(\frac{\mu_F}{\hbar\omega_z}\right) + \frac{1}{2}\left(\frac{\mu_F}{\hbar\omega_z} - 1\right)^2 \theta\left(\frac{\mu_F}{\hbar\omega_z} - 1\right)\right], \tag{A7}$$

where $\mu_F = \mu - \hbar\omega_z/2$ is the chemical potential minus the ground-state harmonic energy along the z axis.

Equation (A7) can be easily inverted and we find

$$\mu_F = \hbar\omega_z \times \begin{cases} 2\pi n_F a_{zF}^2 & \text{for } 0 \leqslant n_F a_{zF}^2 < \dfrac{1}{2\pi}, \\ \sqrt{4\pi n_F a_{zF}^2 - 1} & \text{for } n_F a_{zF}^2 \geqslant \dfrac{1}{2\pi}. \end{cases} \tag{A8}$$

Equation (A8) carries the fermionic nonpolynomial nonlinearity in quasi-2D formulation to be used in Eqs. (7) and (8). In the strict 2D limit, the second term in Eq. (A6) is absent and $\mu_F = 2\pi\hbar\omega_z n_F a_{zF}^2$ corresponding to a cubic nonlinearity.

We can also derive the energy density $\mathcal{E}_F$ of the Fermi gas from the following formula of zero-temperature thermodynamics

$$\mathcal{E}_F = \int dn_F \mu_F(n_F). \tag{A9}$$

In this way we get

$$\mathcal{E}_F = \frac{\hbar\omega_z}{a_{zF}^2} \times \begin{cases} \pi(n_F a_{zF}^2)^2 & \text{for } 0 \leqslant n_F a_{zF}^2 < \dfrac{1}{2\pi}, \\ \dfrac{1}{6\pi}(4\pi n_F a_{zF}^2 - 1)^{3/2} + \dfrac{1}{12\pi} & \text{for } n_F a_{zF}^2 \geqslant \dfrac{1}{2\pi}. \end{cases} \tag{A10}$$

The Fermi gas is strictly 2D only for $0 \leqslant n_F < 1/(2\pi a_{zF}^2)$, i.e., for $0 \leqslant \mu_F < \hbar\omega_z$. For $n_F > 1/(2\pi a_{zF}^2)$, i.e., for $\mu_F > \hbar\omega_z$, several single-particle states of the harmonic oscillator along the z axis are occupied and the gas has the 2D-3D crossover. Finally, for $n_F \gg 1/(2\pi a_{zF}^2)$, i.e., for $\mu_F \gg \hbar\omega_z$, the Fermi gas becomes 3D [51].

The equations of state (A8) and (A10) can be used to write down, in the local density approximation, the density functionals of the quasi-2D Fermi gas in presence of an additional external potential $V(\rho)$ in the cylindric radial direction ρ. In this case the 2D fermionic density n_F becomes a function of the radial coordinate $n_F = n_F(\rho)$.

[1] B. DeMarco and D. S. Jin, Science **285**, 1703 (1999).
[2] K. M. O'Hara, S. L. Hemmer, M. E. Gehm, S. R. Granade, and J. E. Thomas, Science **298**, 2179 (2002).
[3] F. Schreck, L. Khaykovich, K. L. Corwin, G. Ferrari, T. Bourdel, J. Cubizolles, and C. Salomon, Phys. Rev. Lett. **87**, 080403 (2001); A. G. Truscott, K. E. Strecker, W. I. McAlexander, G. B. Partridge, and R. G. Hulet, Science **291**, 2570 (2001).
[4] Z. Hadzibabic, C. A. Stan, K. Dieckmann, S. Gupta, M. W. Zwierlein, A. Gorlitz, and W. Ketterle, Phys. Rev. Lett. **88**, 160401 (2002).
[5] G. Modugno, G. Roati, F. Riboli, F. Ferlaino, R. J. Brecha, and M. Inguscio, Science **297**, 2240 (2002).
[6] G. Roati, F. Riboli, G. Modugno, and M. Inguscio, Phys. Rev. Lett. **89**, 150403 (2002).
[7] K. E. Strecker, G. B. Partridge, and R. G. Hulet, Phys. Rev. Lett. **91**, 080406 (2003); Z. Hadzibabic, S. Gupta, C. A. Stan, C. H. Schunck, M. W. Zwierlein, K. Dieckmann, and W. Ketterle, *ibid.* **91**, 160401 (2003).
[8] R. Roth, Phys. Rev. A **66**, 013614 (2002).
[9] K. Molmer, Phys. Rev. Lett. **80**, 1804 (1998).
[10] R. Roth and H. Feldmeier, Phys. Rev. A **65**, 021603(R) (2002); T. Miyakawa, T. Suzuki, and H. Yabu, *ibid.* **64**, 033611 (2001).
[11] Y. Takeuchi and H. Mori, Phys. Rev. A **72**, 063617 (2005).
[12] Z. Akdeniz, A. Minguzzi, P. Vignolo, and M. P. Tosi, Phys. Lett. A **331**, 258 (2004); P. Capuzzi, A. Minguzzi, and M. P. Tosi, Phys. Rev. A **68**, 033605 (2003).
[13] M. Modugno, F. Ferlaino, F. Riboli, G. Roati, G. Modugno, and M. Inguscio, Phys. Rev. A **68**, 043626 (2003); X.-J. Liu, M. Modugno, and H. Hu, *ibid.* **68**, 053605 (2003).
[14] P. Capuzzi, A. Minguzzi, and M. P. Tosi, Phys. Rev. A **69**, 053615 (2004); **67**, 053605 (2003).
[15] A. Minguzzi, P. Vignolo, M. L. Chiofalo, and M. P. Tosi, Phys. Rev. A **64**, 033605 (2001).
[16] S. K. Adhikari, Phys. Rev. A **70**, 043617 (2004).
[17] S. K. Adhikari, New J. Phys. **8**, 258 (2006).
[18] C. A. Stan, M. W. Zwierlein, C. H. Schunck, S. M. F. Raupach, and W. Ketterle, Phys. Rev. Lett. **93**, 143001 (2004); S. Inouye, J. Goldwin, M. L. Olsen, C. Ticknor, J. L. Bohn, and D. S. Jin, *ibid.* **93**, 183201 (2004).
[19] S. K. Adhikari, Phys. Rev. A **73**, 043619 (2006); S. K. Adhikari and B. A. Malomed, *ibid.* **74**, 053620 (2006).
[20] C. Ospelkaus, S. Ospelkaus, K. Sengstock, and K. Bongs, Phys. Rev. Lett. **96**, 020401 (2006).
[21] M. Zaccanti, C. D'Errico, F. Ferlaino, G. Roati, M. Inguscio, and G. Modugno, Phys. Rev. A **74**, 041605(R) (2006); S. Ospelkaus, C. Ospelkaus, L. Humbert, K. Sengstock, and K. Bongs, Phys. Rev. Lett. **97**, 120403 (2006).
[22] R. J. Donnelly, *Quantized Vortices in Helium II* (Cambridge University Press, Cambridge, 1991).
[23] S. K. Adhikari, Am. J. Phys. **54**, 362 (1986).
[24] K. W. Madison, F. Chevy, W. Wohlleben, and J. Dalibard, Phys. Rev. Lett. **84**, 806 (2000); M. R. Matthews, B. P. Anderson, P. C. Haljan, D. S. Hall, C. E. Wieman, and E. A. Cornell, *ibid.* **83**, 2498 (1999).
[25] D. L. Feder, C. W. Clark, and B. I. Schneider, Phys. Rev. Lett. **82**, 4956 (1999).
[26] B. Jackson, J. F. McCann, and C. S. Adams, Phys. Rev. A **61**, 013604 (1999).
[27] R. J. Marshall, G. H. C. New, K. Burnett, and S. Choi, Phys. Rev. A **59**, 2085 (1999).
[28] L. Dobrek, M. Gajda, M. Lewenstein, K. Sengstock, G. Birkl, and W. Ertmer, Phys. Rev. A **60**, R3381 (1999).
[29] A. A. Svidzinsky and A. L. Fetter, Phys. Rev. A **62**, 063617 (2000); A. L. Fetter and A. A. Svidzinsky, J. Phys.: Condens.

Matter **13**, R135 (2001).
[30] D. S. Rokhsar, Phys. Rev. Lett. **79**, 2164 (1997).
[31] L. Salasnich, A. Parola, and L. Reatto, Phys. Rev. A **59**, 2990 (1999); A. Parola, L. Salasnich, R. Rota, and L. Reatto, *ibid.* **72**, 063612 (2005); L. Salasnich, A. Parola, and L. Reatto, *ibid.* **74**, 031603 (2006).
[32] M. Modugno, C. Tozzo, F. Dalfovo, Phys. Rev. A **74**, 061601(R) (2006); S. Schwartz, M. Cozzini, C. Menotti, I. Carusotto, P. Bouyer, and S. Stringari, New J. Phys. **8**, 162 (2006).
[33] T. Karpiuk, M. Brewczyk, and K. Rzazewski, J. Phys. B **35**, L315 (2002); **36**, L69 (2003).
[34] L. Salasnich, S. K. Adhikari, and F. Toigo, Phys. Rev. A **75**, 023616 (2007).
[35] S. K. Adhikari, Phys. Rev. A **72**, 053608 (2005).
[36] S. K. Adhikari, J. Phys. B **38**, 3607 (2005); Laser Phys. Lett. **3**, 605 (2006).
[37] T. Karpiuk, K. Brewczyk, S. Ospelkaus-Schwarzer, K. Bongs, M. Gajda, and K. Rzazewski, Phys. Rev. Lett. **93**, 100401 (2004).
[38] L. P. Pitaevskii and S. Stringari, *Bose-Einstein Condensation* (Oxford University Press, Oxford, 2003); F. Dalfovo, S. Giorgini, L. P. Pitaevskii, and S. Stringari, Rev. Mod. Phys. **71**, 463 (1999); V. I. Yukalov, Laser Phys. Lett. **1**, 435 (2004); V. I. Yukalov and M. D. Girardeau, *ibid.* **2**, 375 (2005).
[39] E. Lipparini, *Modern Many-Particle Physics: Atomic Gases, Quantum Dots and Quantum Fluids* (World Scientific, Singapore, 2003).
[40] L. Salasnich, Laser Phys. **12**, 198 (2002); L. Salasnich, A. Parola, and L. Reatto, Phys. Rev. A **65**, 043614 (2002).
[41] L. Salasnich, A. Parola, and L. Reatto, Phys. Rev. A **69**, 045601 (2004); **70**, 013606 (2004); **72**, 025602 (2005).
[42] M. Girardeau, J. Math. Phys. **1**, 516 (1960); M. Girardeau, Phys. Rev. **139**, B500 (1965); L. Tonks, Phys. Rev. **50**, 955 (1936); G. E. Astrakharchik, D. Blume, S. Giorgini, and B. E. Granger, J. Phys. B **37**, S205 (2004).
[43] Z. Idziaszek and T. Calarco, Phys. Rev. A **71**, 050701(R) (2005).
[44] M. Olshanii, Phys. Rev. Lett. **81**, 938 (1998); D. S. Petrov, M. Holzmann, and G. V. Shlyapnikov, *ibid.* **84**, 2551 (2000); D. S. Petrov and G. V. Shlyapnikov, Phys. Rev. A **64**, 012706 (2000); B. Tanatar, A. Minguzzi, P. Vignolo, and M. P. Tosi, Phys. Lett. A **302**, 131 (2002).
[45] D. M. Jezek, M. Barranco, M. Guilleumas, R. Mayol, and M. Pi, Phys. Rev. A **70**, 043630 (2004).
[46] M. Pi, X. Viñas, F. Garcias, and M. Barranco, Phys. Lett. B **215**, 5 (1988).
[47] L. Salasnich and B. A. Malomed, Phys. Rev. A **74**, 053610 (2006).
[48] S. K. Adhikari and P. Muruganandam, J. Phys. B **35**, 2831 (2002); P. Muruganandam and S. K. Adhikari, *ibid.* **36**, 2501 (2003).
[49] S. K. Adhikari, Phys. Rev. A **65**, 033616 (2002); Phys. Rev. E **65**, 016703 (2002); F. Dalfovo and S. Stringari, Phys. Rev. A **53**, 2477 (1996); F. Dalfovo and M. Modugno, *ibid.* **61**, 023605 (2000).
[50] S. K. Adhikari, Phys. Rev. A **63**, 043611 (2001).
[51] L. Salasnich, J. Math. Phys. **41**, 8016 (2000).